Real-time Implementation of Optimal Power Flow Calculator for HVDC Grids

Muhammad Hassan Fidai[*]**, Davood Babazadeh**[*]**, Jonathan Hanning**[†]**,
Tomas X. Larsson**[†]**, Lars Nordström**[*]

**[*] Industrial Information & Control Systems, School of Electrical Engineering, KTH-
Royal Institute of Technology, SE-100 44, Stockholm, Sweden
[†] DC Grids Simulation Center, ABB AB, 721 83 Västerås, Sweden**

**E-mail: fidai@kth.se, davood@kth.se, jonathan.hanning@se.abb.com,
tomas.x.larsson@se.abb.com, larsn@ics.kth.se**

SUMMARY

The aim of the paper is to present the centralized architecture for power balancing management in an HVDC, High Voltage Direct Current, grid connecting different AC areas with high penetration of variable energy resources. Such a centralized high level DC Supervisory Control (DCSC) that functions in slower time scale compared to outer level controller has been evaluated in a real time co-simulation test-bed. The test platform includes OPAL-RT's eMEGAsim real time simulator to model the power system, the ABB's industrial HVDC controller (MACH), real time communication simulator OPNET to model the communication network and finally the DCSC application which is implemented on a Linux machine. The DCSC consists of a network topology manager to identify the grid configuration and employs an Optimal Power Flow (OPF) calculator based on interior point optimization method to determine the set-point values for all HVDC stations in a grid. The OPF calculator takes into account the DC voltage, converter and DC line constraints. The performance of the DC supervisory control has been tested for various test cases for a 7-terminal HVDC grid. Test cases include I) Variable power generation from wind farms, II) Station disconnection and III) DC grid islanding. Besides, the proper sampling rate has been chosen and justified to show the benefit of frequent updating of set-point compared to letting the DC droop control scheme take over the mismatch in the system. The results of different test cases show that a DCSC can improve the power extraction from wind farms by updating the set-points following any change in the system. Using a 3.2 GHz machine, it approximately takes 15 ms for the DCSC to converge to a proper solution and send the updated set-points.

KEYWORDS

Optimal power flow, Real-time simulations, Supervisory control, VSC-HVDC grid.

INTRODUCTION

Integration of renewable resources such as remote solar or wind farms and electric power trading between neighbouring countries lead to new requirements on the development of the transmission grids. Since AC grid expansion is limited by legislations issues, HVDC technology with its diverse benefits compared to AC is being considered as appropriate alternative solution. HVDC technology is being used to transmit power over long distances and to connect different AC systems for past six decades. Line Commutated Converters (LCC) and Voltage Source Converters (VSC) are the two HVDC technologies currently available. The latter has significant advantages over LCC when it comes to integration of off-shore wind energy [1] or to provide reactive power support to the connecting AC system [2]. A VSC-HVDC grid has been proposed in the literature [3, 4, 5, 6] to overcome the aforementioned challenges. Such an HVDC grid can be augmented or integrated within single or different AC systems.

Due to the versatile nature of future applications, different solutions have been suggested for building HVDC grids. Its various aspects with the technological and economical perspectives have been addressed in the literature which includes but are not limited to different grid topologies, protection schemes and detailed control strategies [7, 8]. Various control schemes have been presented, where some advocate distributed control strategy [7], others address the problem with a centralized control scheme [9] [10].

The developed HVDC grid can be either embedded inside one AC grid or connecting several AC areas. Variable power injection from wind farms, varying active and reactive power requirements of the connecting AC systems and changes in the grid topologies due to faults are the major challenges in the balanced, stable and reliable operation of the HVDC grid. In both the distributed and centralized architectures, a separate DC supervisory control can be proposed to control the HVDC grids using the interfacing information from the AC SCADA(s) (Supervisory Control And Data Acquisition). The supervisory control is supposed to calculate the OPF in order to run the system in the most optimal situation. Based on the architecture, the required information, the boundaries of the system and also objective function can vary.

Various techniques have been developed and are discussed in the literature for OPF of an HVDC grid. Most of the work has been carried out on the combined AC/DC load flow and can be subdivided into unified and sequential methods. In the unified approach both AC and DC system equations are solved simultaneously [9], whereas in the sequential method, first AC system equations are solved and then the DC system equations [10].

The fundamental component of any OPF scheme is its optimization solver. Different optimization approaches have been presented in the literature for DC OPF. A second order cone programming formulation of the AC/DC power flow problem has been presented [11], which is solved using interior point optimization method. [12] also presents the use of interior point optimization method for OPF. Different optimization solvers for combined AC/DC power flow are tested by [13] and IPOPT has been declared to provide the best results. An IPOPT solver uses an interior point line search filter method and is commonly used in solving large-scale nonlinear optimization problems [14].

This paper presents a centralized control scheme for HVDC grids. The implemented DCSC only considers the DC system for the formulation of the OPF problem and employs IPOPT optimization solver for its solution. For testing and validation, DCSC is integrated in a real-time co-simulation platform. The HVDC grid has been simulated in OPAL-RT real-time environment whereas communication network is emulated in OPNET [15].

HVDC GRID

HVDC grids comprise several VSC converters that connect different AC areas through a DC meshed network (see Fig. 1).These connected AC areas can be operated by different transmission system operators (TSOs). Secure operation and control of this hybrid AC/DC grid needs a multilayer control system to manage different functions such as voltage or power flow control.
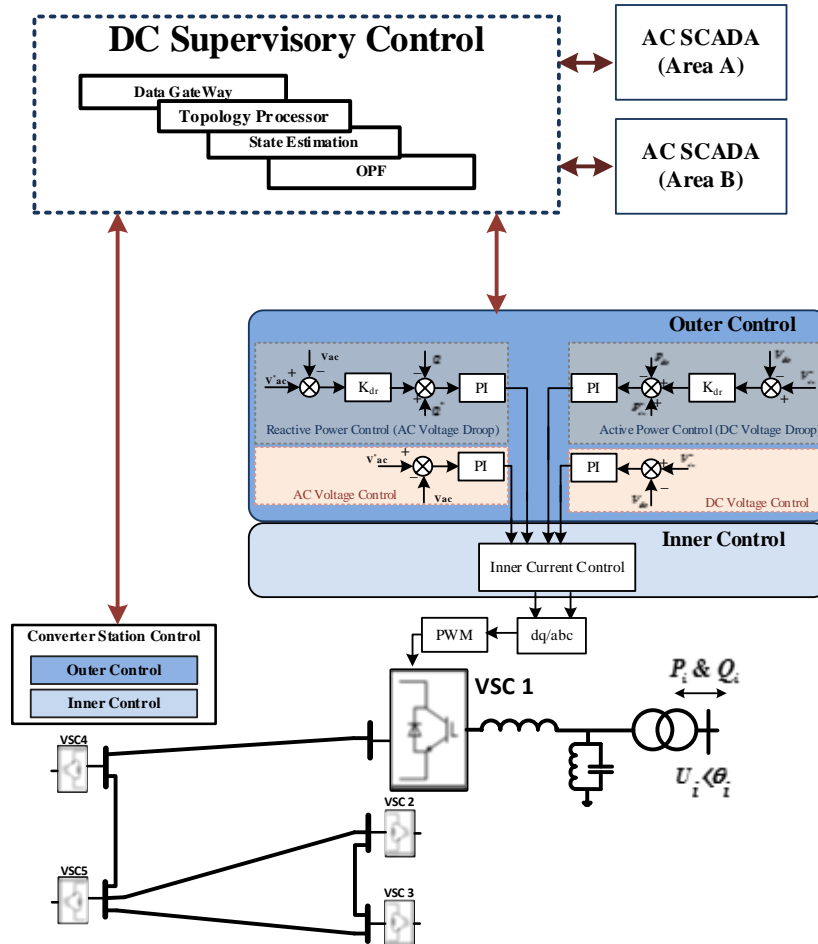

Figure 1, HVDC grid control architecture

A. Control Layers

The HVDC grid control system can be separated into two different levels; supervisory control level and converter station level. Each level, in turn, is divided into specific functional layers. The converter station level contains two layers of inner controller and outer controller (see Fig. 1). The dynamic of control functions implemented in each layer becomes slower when it goes from lower levels to upper levels. The phenomena within inner or outer control layers take place in the range of respectively milliseconds and several of milliseconds to seconds. Based on communication infrastructure, control functions within the supervisory level can vary from tens of milliseconds for wide area protection system to minutes or longer for tertiary power flow control. Supervisory control functions for HVDC grid can be deployed in separate DCSCs or be integrated into the AC SCADA. A typical centralized control system for HVDC grid with its corresponding control levels are depicted in Fig. 1.

Inner control layer: Vector control as one of different approaches introduced for the control of VSC sets the converter to work as a controllable current source [16]. In this approach, the

3

injected current vector is set to follow a reference current vector. Therefore, each VSC needs to have an internal current controller. In this scheme, *dq* reference frame is used in order to project current vector into *d* and *q* axes (i.e. i_d and i_q) and respectively, decouple the control of active and reactive power.

Outer control layer: The outer controller can control reactive power (or AC voltage) on the AC side and active power (or DC voltage) on the DC side. The outer controller provides the inner controller with the reference current values in *dq* coordinates. This controller is slower than the inner controller and has separate loops for station active power and reactive power control. Various control modes are available for the station active power control loop. Due to its simplicity, usually a PI controller is used which tries to track either the PCC active power or DC voltage set-point. The former is known as constant active power control mode whereas the latter is known as constant DC voltage control mode.

In a grid configuration there will be one DC voltage controlling station (i.e. slack bus) which strives to maintain constant DC voltage according to reference values. The other stations can be either in active power control mode, implying that they strive to maintain constant active power according to their reference values or alternatively some of the converters in the grid can be assigned also to change the injected active power proportional to the local deviation of DC voltage in order to provide the active power balance in the HVDC grid. This control method is known as DC voltage droop that is completely communication free during the operation. This method is more suitable for the HVDC grid connected with variable resource such as large-scale offshore wind farms. This fast DC voltage droop control helps converters to manage the power mismatch similar to frequency control in AC system but without any accurate power sharing assignment for converters. However for accurate power sharing assignments in the whole grid, higher level power injection coordination is still needed to define the new optimal set-points. In this case the droop setting and/or new set-points can be calculated by DCSC every few seconds or minutes and then be sent to converters.

DC SUPERVISORY CONTROL

The DCSC provides the control strategy for the coordination of VSC-HVDC terminals connected in a grid configuration. It responds to the contingencies on the AC and DC sides, and periodically computes the set-point references for the station control system. The DCSC also optimizes the post contingencies set points to minimize the losses in the system.

DCSC bridges the gap between the power schedule which is usually received from the SCADA and has a time scale of tens of minutes and relatively fast balancing operation in the grid. The schedule is the input to the DCSC received from SCADA. It may be defined based on operator manual input, or on the output of an OPF or market dispatch algorithm. A schedule is generally not feasible, i.e., an attempt at operating perfectly on schedule may introduce overloads or power mismatches at some nodes because of inaccuracies in the model used when computing the schedule or due to change in operating conditions. Another source of mismatch is uncertainty in models and parameters of the DC stations and lines which will introduce inaccuracy in the loss calculation. The DCSC computes the new operational set-points trying to track the schedule as much as possible, meanwhile minimizing the system losses. Depending on the outer layer active power control mode of the VSC station, DCSC assigns it a power or voltage priority according to the table I. For stations with the power priority DCSC tracks its PCC active power schedule whereas DC voltage schedule is tracked for stations with the voltage priority. The extent to which the DCSC follows the schedule of a station is specified by the power or voltage cost assigned to it. Hence the objective function, $f(x)$ to be minimized by the DCSC becomes

$$f(x) = \sum_{i=1}^{n_{conv}} C_{p,i}\left(P_i^{dc} - P_i^{sched}\right)^2 + C_{v,i}\left(V_i^{dc} - V_i^{sched}\right)^2 + \sum_{i=1}^{n_{conv}} P_{loss,i}$$

where, n_{conv} is the total number of converters in the grid. $C_{p,i}$ and $C_{v,i}$ are the cost of deviation from the power, P_i^{sched} and voltage, V_i^{sched} schedule values respectively. P_i^{dc} and V_i^{dc} are the optimal DC power and voltage setpoints respectively to be calculated and P_{loss} represents the losses in the system. The operational limitations supported by the DCSC are HVDC grid voltage limits, HVDC grid branch current limits, DC converter voltage and current limits and AC voltage and current limits. DCSC formulates a nonlinear constrained optimization problem of the form

$$\min f(x)$$
$$such\ that\ g(x) = b_{eq}$$
$$b_{ineq} \leq h(x) \leq b_{ineq}$$
$$LB \leq x \leq UB$$

The lower bound, LB, and upper bound, UB of the optimization variables are defined by the HVDC grid voltage and power limitations. The power balance in the HVDC grid network gives rise to the linear equality, b_{eq} and inequality, b_{ineq} constraints. Nonlinear inequality constraints of the optimization problem are specified by the DC branch current and AC system capabilities limits.

Table I, Priority mode for DCSC

Station control mode	Priority
Constant PCC active power control	Power
Constant DC voltage control	Voltage
Droop control mode	Power

PROOF OF CONCEPT

A. Simulation Platform

The electric power grid is a large complex system that includes the coordination of different support systems such as information and communication tools used for monitoring, operation and protection. To ensure the secure operation of the entire system, a detailed study of all such composing systems is necessary. Real-time simulation tools offer a cost-effective and safe approach to assess the performance of possible solutions. Numerous power systems and information and communication technology co-simulation platforms have been proposed in the literature [15, 17].

The DCSC continuously exchanges data with the VSC stations in the grid and the decisions are made based on the real time measurements received by the DCSC. The accuracy, resolution and latency of these measurements have a direct correlation with the performance of the DCSC. Hence the presented DCSC is tested and validated with in a real-time co-simulation platform. The simulation platform including a DCSC implemented on a Linux machine is shown in Fig. 2.

A multi terminal VSC-HVDC grid is simulated in an OPAL-RT real-time simulator. Three of the VSC terminals in the simulated grid are emulated by physical ABB VSC-HVDC controllers, which exchange measurements with the simulated HVDC grid model via analogue input/output modules of OPAL-RT. Each of these controllers communicate with the DCSC (Linux Machine) using Ethernet protocol, through a communication simulator which emulates the respective, controlled VSC-HVDC terminals to be in different geographical location from a communication network standpoint. Measurements to and from all the other VSC-HVDC terminals and the network topology information

of the simulated HVDC grid are exchanged directly between the DCSC and OPAL-RT via UDP communication link.
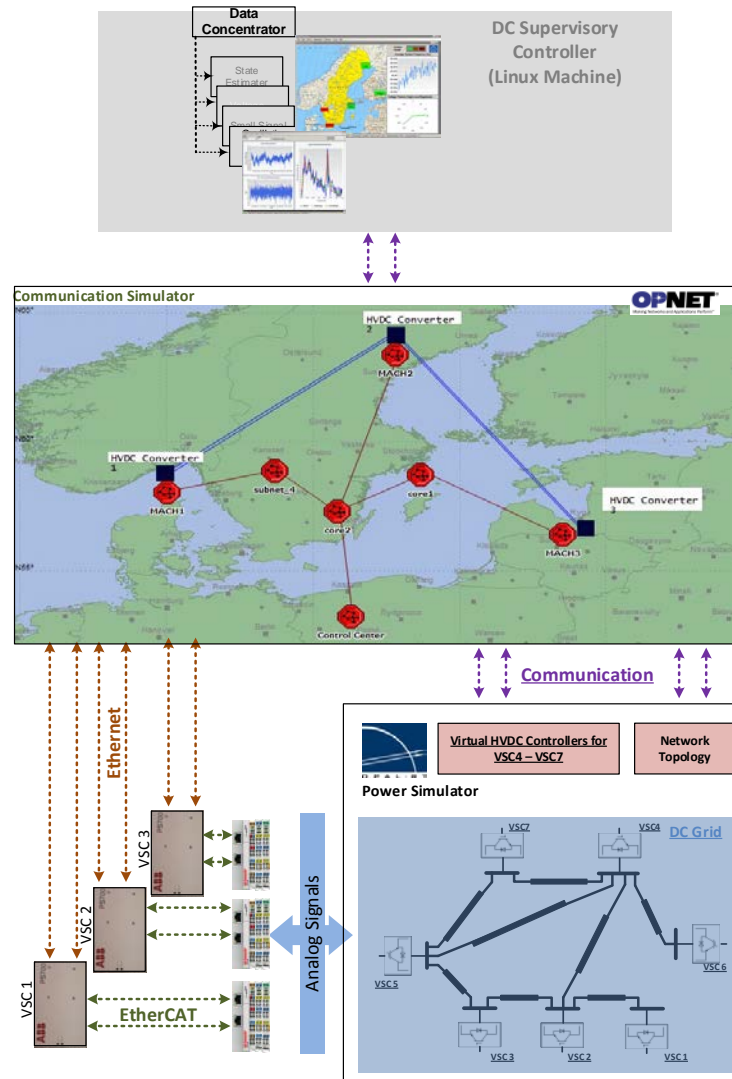

Figure 2, Simulation platform for DCSC

Based on communication infrastructure and available DC measurement unit specification, it is possible to have high sampling frequency to be able to monitor the system more accurately at the control center. The sampling rate does not introduce any requirement on the DCSC to run the OPF at each sample; rather it makes the whole process more observable for the DCSC. OPF calculations can be run every few minutes based on AC sampling frequency or quite fast on the order of few seconds or even milliseconds depending on the requirements dictated by the operational strategy of DC or AC/DC transmission operator. In this study the system is sampled every 5 seconds by the DCSC, which does not need fast communication and process.

The uncertainty and variation of wind production can be one of the key parameters to define the resolution of change in power which actuates the OPF of the DCSC. The study on the historical wind data from available databases such as Belgian or Pacific North-west wind production shows that the generation can vary up to 1.6% of total capacity per minute. Such variation for large-scale offshore wind farms connected to HVDC grid can be managed securely by DC voltage droop control scheme [18]. Hence the DCSC only runs an OPF and computes new set-points when there is power a mismatch of more than 3% or if there is a change in grid configuration.

B. VSC-HVDC grid model

A 7-terminal VSC-HVDC Grid model [19] has been simulated in OPAL-RT simulator and is shown in Fig. 3. The simulated grid is uni-polar and an average model is used for each VSC-HVDC station.

VSC1 and 6 are assumed to be connected with offshore wind farms. In order to simulate the DC line fault scenarios leading to line disconnection, ideal switches are installed on the DC lines in the model. Parameters and the control modes of each VSC-HVDC terminal are shown in table II, whereas as the DC line parameters are shown in table III.
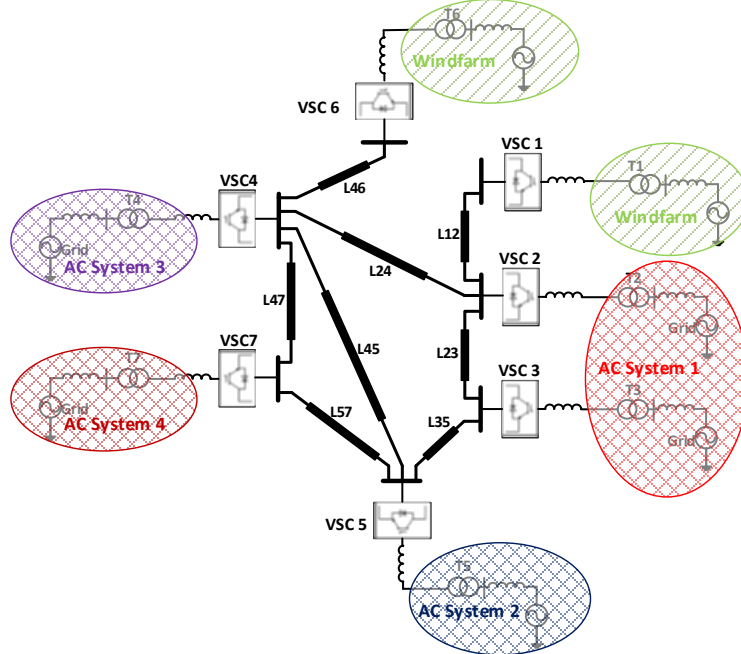

Figure 3, 7-Terminal VSC HVDC model simulated in OPAL-RT

Table II, VSC terminals power ratings and control modes

Terminal	Power Rating [MW]	Control Mode
VSC1	200	Constant PCC active power
VSC2	300	Droop Control
VSC3	150	Droop Control
VSC4	200	Droop Control
VSC5	300	Constant DC Voltage
VSC6	100	Constant PCC active power
VSC7	50	Droop Control

Table III, HVDC Grid line parameters

Lines	Distance [km]	Resistance [Ohm]	Inductance [mH]	Maximum Current [kA]
L12	413	5	43.6	1
L23	248	3	26.2	0.5
L24	207	2.5	21.9	1
L35	331	4	35.0	1
L45	83	1	8.76	0.5

L46	207	2.5	21.9	0.5
L47	289	3.5	30.5	0.5
L57	165	2	17.4	0.5

C. Results

The simulated HVDC grid model described in the section above is tested with DCSC for various scenarios. For all scenarios, VSC stations are operated at a maximum of 80% of their rated power.

1) Scenario 1: Variable power generation

To test the capability of DCSC to maximize the power output from wind farms and to validate its ability to maintain balanced power operation in the grid, the generation from wind farm connected with VSC 1 is varied. Results are gathered for simulations ran with and without the DCSC. Results shown in Fig. 4 are presented in form of a difference in VSC stations, measured PCC active power and the schedule value. Variation in power generation has maximum toll on VSC 5 since it is in voltage control mode. However, the droop control of all the other stations also contribute to balance out the power mismatch in the system as can be seen from the plot of VSC 2. When the system is operated with DCSC, it can be seen that after 5 seconds of each power variation, DCSC corrects the set-point of stations in droop control and transfers all the power difference to VSC 5 since it has the least cost to follow the power schedule. Plots for all the VSC stations with DCSC are shown in Fig. 5.
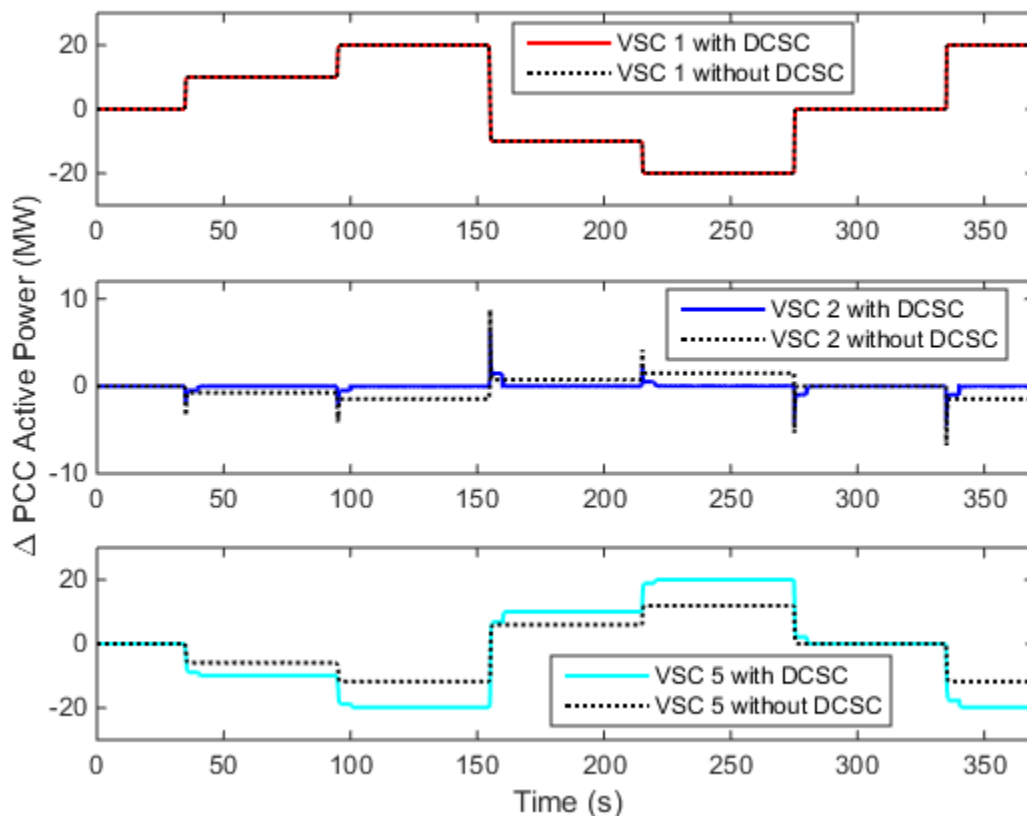

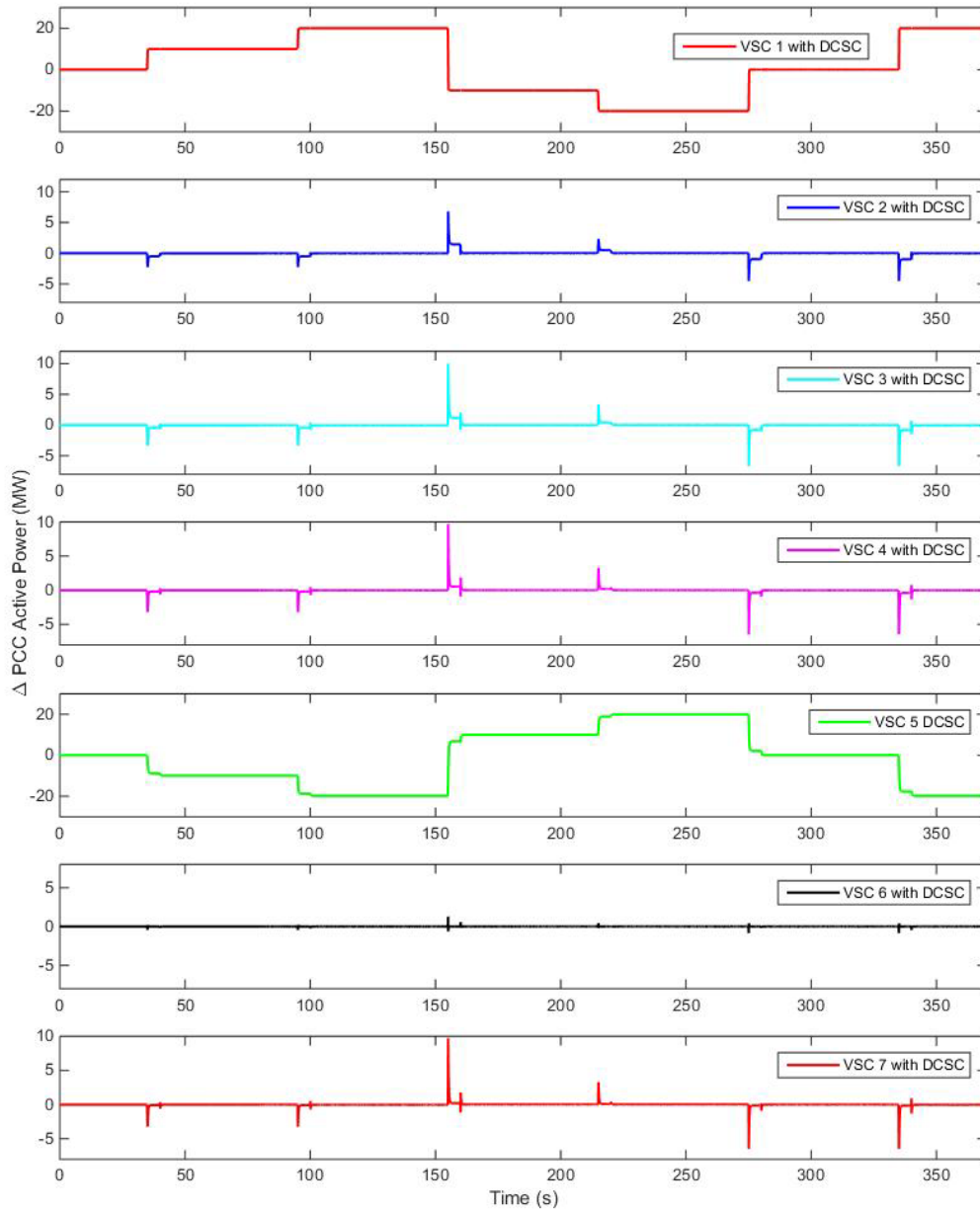**Figure 4, Results for scenario1, Difference in active power of VSC stations**

Figure 5, Results for scenario 1 with DCSC

2) Scenario 2: Station disconnection

In the case of fault in a VSC, the converter is disconnected from the HVDC grid. To test the response of the DCSC in such an event the HVDC grid model is simulated such that VSC1 is disconnected. The simulation is run twice. Once with all the stations in droop control mode having the same cost $C_{p,3} = 1$, shown in Fig. 6, and once with VSC 3 having $C_{p,3} = 0$ shown in Fig. 7. In both cases for VSC5 $C_{p,5} = 1$, since it is in voltage control mode. In the former case all the imbalance of power is accounted for by VSC5 whereas for the later it is shared between VSC5 and VSC3, validating that DCSC follows the schedule of the station based on its assigned cost.
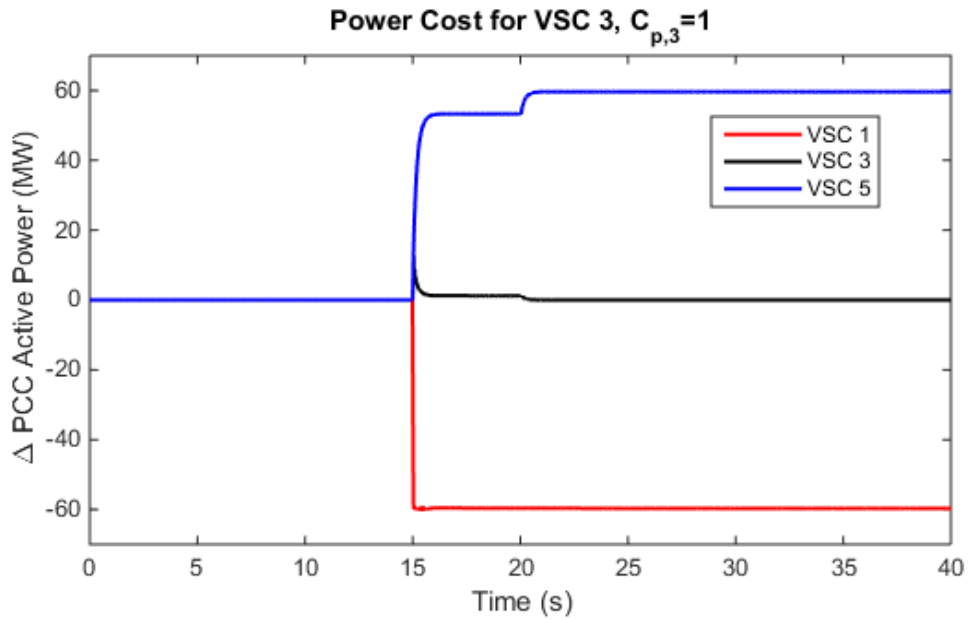
9

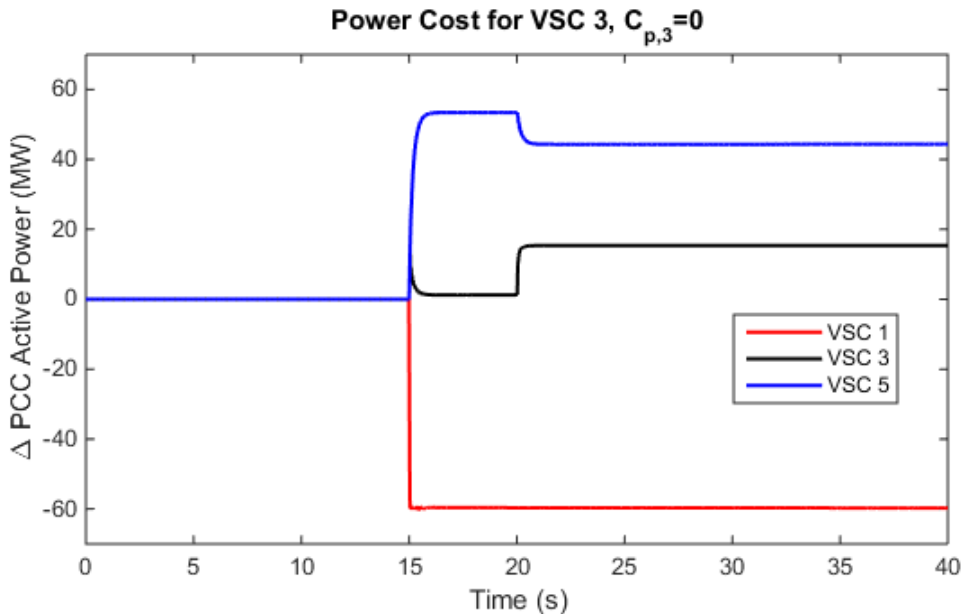**Figure 6, Results for scenario 2, VSC 3 has same power cost $C_{p,3}1$**

Figure 7, Results for scenario 2, VSC 3 has lower power cost $C_{p,3} = 0$

3) Scenario 3: Islanding

Line faults in an HVDC grid at times can lead to creation of multiple sub systems. The operation of DCSC is tested for such a scenario where a simulation is carried out such that the lines L_{24} and L_{35} of the grid shown in Fig. 3 are disconnected leading to the creation of two subsystems. VSC1 to VSC3 constitute one system assumed as subsystem A. VSC4 to VSC7 constitute another system assumed to be subsystem B. The results of the simulation are presented in Fig. 8 and 9 which show the plots of subsystem A and B respectively. The islanding occurs 40 s after both subsystems have a totally decoupled operation. Generation from VSC1 is varied between 50 s and 250 s. Since subsystem A lacks a slack bus the power mismatch is shared by the droop control of VSC 2 and VSC 3. In contrast to subsystem A, subsystem B has a slack bus (VSC 5) which maintains the power balance when the generation from VSC 6 is varied between 250 s and 400 s.
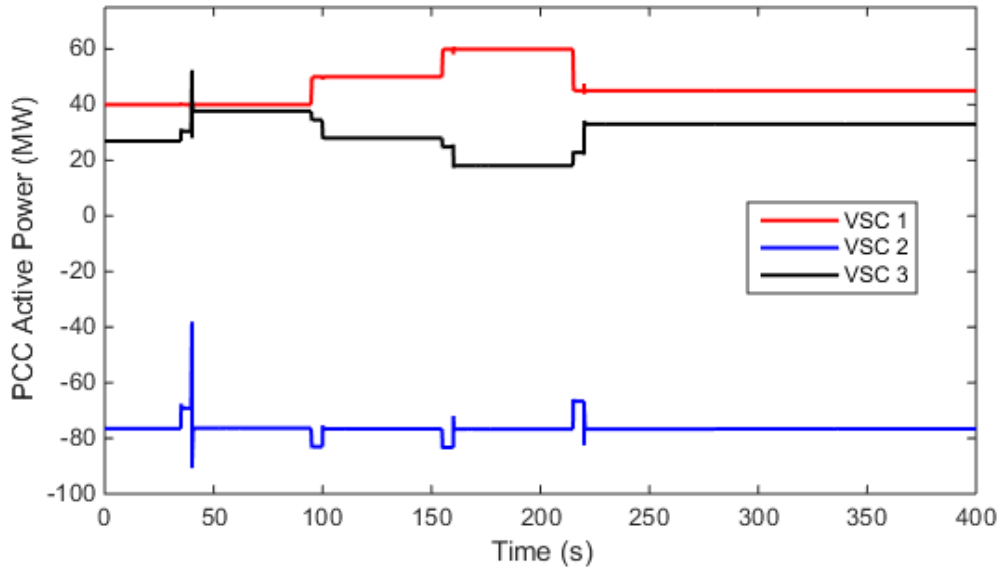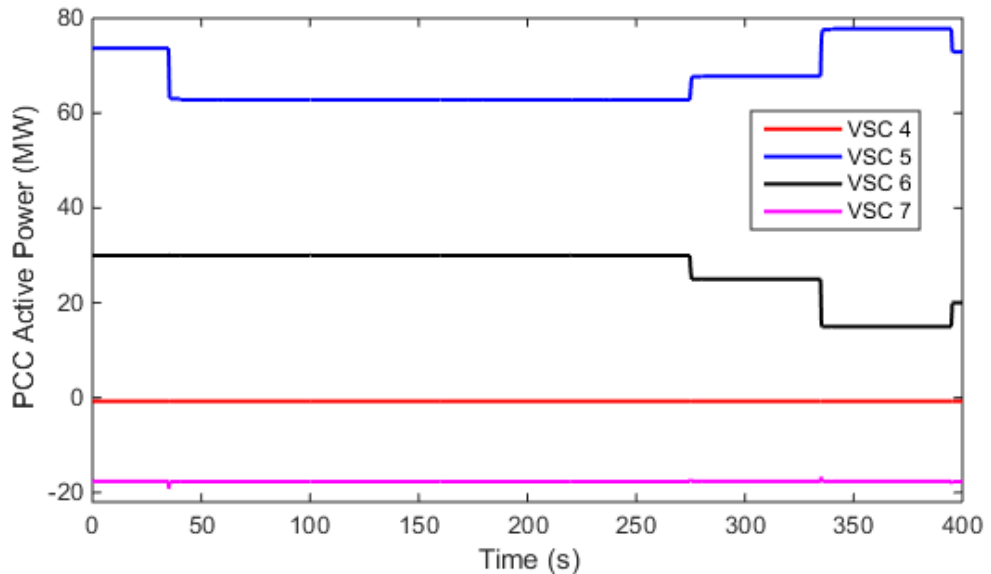
Figure 8, Results for scenario 3, Subsytem A

Figure 9, Results for scenario 3, Subsytem B

CONCLUSION

The presented and implemented version of a DCSC has shown satisfactory results during its testing and validation within the co-simulation platform. The results show that the DCSC improves the power sharing from wind farms by updating the set-points following any change in the system. Moreover the DCSC ensures the grid operation within the operational constraints at all times. Using 3.2 GHz machine, it takes approximately 15 ms for the DCSC to converge to a proper solution and send the updated set-points. Considering the variety of test cases, the original OPF calculator could have been modified to deal with the transient conditions in more robust way. Although in the case of islanding, the current algorithm is not designed to identify separate islands and reassign required control modes such as new slack bus, but the station set-points necessary for the stable operation of individual islands can be calculated. Islanding identification, logical operational reassignments of the converter modes

11

and corresponding multi-area OPF calculations has been considered as part of the further work.

BIBLIOGRAPHY

[1] N. Flourentzou, V. Agelidis, and G. Demetriades, "VSC-based HVDC power transmission systems: An overview," *IEEE Transactions on Power Electronics,* vol. 24, no. 3, pp. 592-602, March 2009.

[2] Lidong Zhang, Lennart Harnefors, Pablo Rey, "Power system reliability and transfer capability improvement by VSC-HVDC," in *Security and reliability of electric power systems, Cigre regional meeting*, Tallin, Estonia, June 2007.

[3] "VSC transmission," Cigre Working Group B4.37-269, 2005.

[4] G. Asplund, K. Eriksson, and H. Jiang, "DC transmission based on voltage source converters," in *Cigre Colloquium on HVDC and FACTS*, South Africa, 1997.

[5] S. Johansson, G. Asplund, E. Jansson, and R. Rudervall, "Power system stability benefits with VSC DC-transmission systems," in *Cigre Conference B4-204*, 2004.

[6] L. Zhang, L. Harnefors, and P. Rey, "Power system reliability and transfer capability improvement by VSC-HVDC (HVDC light)," in *Cigre Regional Meeting*, 2007.

[7] J. Beerten, D. Van Hertem, and R. Belmans, "VSC MTDC systems with a distributed DC voltage control - a power flow approach," *IEEE PES Trondheim PowerTech ,* pp. 1-6, June 2011.

[8] D. Babazadeh, M. Chenine, L. Nordström, "Survey on the factors required in design of communication architecture for future DC grids," vol. 2, no. 1, pp. 58-63, 2013.

[9] M. El-Marsafawy and R. Mathur, "A new, fast technique for load-flow solution of integrated multi-terminal DC/AC systems," *IEEE Transactions on Power Apparatus and Systems,* Vols. PAS-99, no. 1, p. 246255, Jan 1980.

[10] M. El-Hawarya, S. T. Ibrahiml, "A new approach to AC-DC load flow analysis," *Electric Power Systems Research,* vol. 33, pp. 193-200, June 2004.

[11] M. Baradar, M. Hesamzadeh, and M. Ghandhari, "Second-order cone programming for optimal power flow in VSC-type AC-DC grids," *IEEE Transactions on Power Systems,* vol. 28, no. 4, pp. 4282-4291, Nov. 2013.

[12] J. Momoh, M. El-Hawary, and R. Adapa, "A review of selected optimal power flow literature to 1993. II. Newton, linear programming and interior point methods," *IEEE Transactions on Power Systems,* vol. 14, no. 1, pp. 105-111, Feb. 1999.

[13] W. Feng, A. L. Tuan, L. Tjernberg, A. Mannikoff, and A. Bergman, "A new approach for benefit evaluation of multiterminal VSC HVDC using a proposed mixed AC/DC optimal power flow," *IEEE Transactions on Power Delivery,* vol. 29, no. 1, pp. 432-443, Feb 2014.

[14] Andreas Wächter, Lorenz T Biegler, "On the Implementation of an Interior-Point Filter Line-Search Algorithm for Large-Scale Nonlinear Programming," IBM Research Report RC 23149 IBM T.J. Watson Research Center, Yorktown Heights, NY. USA, March 2004.

[15] K. Mets, J. Ojea, and C. Develder, "Combining power and communication network simulation for cost-effective smart grid analysis," *IEEE Communications Surveys Tutorials,* vol. 16, no. 3, pp. 1771-1796, March 2014.

[16] T. Haileselassie, "Control, dynamics and operation of multi-terminal VSC-HVDC transmission systems," Ph.D. dissertation, NTNU, December 2009.

[17] J. Nutaro, P. Kuruganti, L. Miller, S. Mullen, and M. Shankar, "Integrated hybrid-simulation of electric power and communications systems," *IEEE Power Engineering Society General Meeting,* pp. 1-8, June 2007.

[18] A. Abdel-khalik, A. Massoud, A. Elserougi, and S. Ahmed, "Optimum power transmission-based droop control design for multi-terminal HVDC of offshore wind farms," *IEEE Transactions on Power Systems,* vol. 28, no. 3, pp. 3401-3409, Aug 2013.

[19] E. Velleux and B. T. Ooi, "Multi-terminal HVDC grid with power flow controllability," B4-301, Cigre, 2012.